Published in final edited form as:
Cancer Res. 2012 February 1; 72(3): 726–735. doi:10.1158/0008-5472.CAN-11-2167.

Sphingosine-1-phosphate produced by sphingosine kinase 1 promotes breast cancer progression by stimulating angiogenesis and lymphangiogenesis

Masayuki Nagahashi[1,2], **Subramaniam Ramachandran**[1,2], **Eugene Y. Kim**[2], **Jeremy C. Allegood**[2], **Omar M. Rashid**[1,2], **Akimitsu Yamada**[1,2], **Renping Zhao**[3], **Sheldon Milstien**[2], **Huiping Zhou**[3], **Sarah Spiegel**[2], and **Kazuaki Takabe**[1,2]

[1]Division of Surgical Oncology, Virginia Commonwealth University School of Medicine

[2]Department of Biochemistry and Molecular Biology, and the Massey Cancer Center, Virginia Commonwealth University School of Medicine

[3]Department of Microbiology and Immunology, Virginia Commonwealth University School of Medicine

Abstract

Sphingosine-1-phosphate (S1P) is a pleiotropic bioactive lipid mediator that promotes breast cancer progression by diverse mechanisms that remain somewhat unclear. Here we report pharmacological evidence of a critical role for sphingosine kinase 1 (SphK1) in producing S1P and mediating tumor-induced hemangiogenesis and lymphangiogenesis in a murine model of breast cancer metastasis. S1P levels increased both in the tumor and the circulation. In agreement, serum S1P levels were significantly elevated in stage IIIA human breast cancer patients, compared to age/ethnicity-matched healthy volunteers. However, treatment with the specific SphK1 inhibitor SK1-I suppressed S1P levels, reduced metastases to lymph nodes and lungs and decreased overall tumor burden of our murine model. Both S1P and angiopoietin 2 (Ang2) stimulated hemangiogenesis and lymphangiogenesis *in vitro* whereas SK1-I inhibited each process. We quantified both processes *in vivo* from the same specimen by combining Directed In Vivo Angiogenesis Assays (DIVAA) with Fluorescence Activated Cell Sorting (DIVAA/FACS), thereby confirming the results obtained *in vitro*. Notably, SK1-I decreased both processes not only at the primary tumor but also in lymph nodes, with peritumoral lymphatic vessel density reduced in SK1-I-treated animals. Taken together, our findings demonstrate that SphK1-produced S1P is a crucial mediator of breast cancer-induced hemangiogenesis and lymphangiogenesis. Our results implicate SphK1 along with S1P as therapeutic targets in breast cancer.

Keywords

sphingosine kinase 1; sphingosine-1-phosphate; lymphangiogenesis; angiogenesis; lymph node metastasis

Corresponding author: Kazuaki Takabe MD PhD FACS, Division of Surgical Oncology, Virginia Commonwealth University School of Medicine and Massey Cancer Center, West Hospital 7-402, 1200 East Broad Street, PO Box 980011, Richmond, Virginia 23298-0011 USA, Tel: 858-945-5405, Fax: (804) 828-4808, ktakabe@vcu.edu.

Disclosure of Potential Conflicts of Interest
No potential conflicts of interest to disclose.

Introduction

Breast cancer is the most commonly diagnosed cancer among women accounting for 30% of all new cancer cases, and close to 40,000 breast cancer deaths are expected to occur among US women in 2011 (1). The majority of deaths of breast cancer patients occur after it metastasizes and becomes a systemic disease (2). To date, most systemic therapies, including cytotoxic chemotherapy, target the tumor itself and not the host tumor microenvironment, which is known to play an important role in progression of cancer (3, 4).

It is well established that hemangiogenesis is one of the key tumor microenvironmental factors in cancer progression. Tumor growth beyond a diameter of a few millimeters requires hemangiogenesis which contributes to the development of metastatic disease (5, 6). Although hemangiogenesis is known to be an acquired capability of cancer (7), results of multiple randomized clinical trials that targeted hemangiogenesis using Bevacizumab, an anti-vascular endothelial growth factor (VEGF) monoclonal antibody, failed to show overall survival benefit in breast cancer (8–10).

Breast cancer first metastasizes to its sentinel lymph node and the level of lymph node metastasis is a major determinant for staging and prognosis of breast cancer (2, 11). Recently, lymphangiogenesis, a process that generates new lymphatic vessels from pre-existing ones, was found to be mediated by several factors including VEGF-C, D and angiopoietins (Ang1 and Ang2), which provided new insights into how the lymphatic vessels grow and affect metastasis (12, 13). Although clinical and experimental evidence suggest a role of lymphangiogenesis in lymph node metastasis, this process is far less understood than hemangiogenesis (13, 14).

The pleiotropic bioactive lipid mediator sphingosine-1-phosphate (S1P) is now emerging as a key regulatory molecule in cancer through its ability to promote cell proliferation, migration, invasion, and hemangiogenesis (15, 16). S1P is generated intracellularly by two sphingosine kinases, SphK1 and SphK2, and is exported out where it regulates many functions by binding to and signaling through a family of five G protein-coupled receptors ($S1P_{1–5}$). This process known as “inside-out” signaling explains the autocrine and paracrine actions of S1P (15). We previously showed that SphK1, but not SphK2, is involved in S1P export from breast cancer cells mediated by the ATP-binding cassette transporters, ABCC1 and ABCG2 (17). Expression of SphK1 is up-regulated in breast cancer (18, 19), correlates with poor prognosis (20), and is associated with resistance to chemotherapy (18). Furthermore, abundant evidence implicates the SphK1/S1P/$S1P_1$ axis in hemangiogenesis and vasculogenesis (21). In contrast, only a few studies so far have examined the involvement of SphK1 and S1P in lymphangiogenesis. S1P has been shown to induce *in vitro* lymphangiogenesis via the $S1P_1$ receptor (22), and it was recently reported that SphK1 and S1P in lymphatic endothelial cells (LECs) are required for proper development of lymphatic vessels (23). However, nothing is yet known of the role of SphK1 and S1P in tumor-induced lymphangiogenesis *in vivo*.

In this study, we utilized an improved syngeneic breast cancer cell implantation method, which models human breast cancer biology better than conventional xenograft subcutaneous implantation, to explore the role of SphK1 and S1P in hem- and lymphangiogenesis. We found not only that circulating S1P levels correlated with tumor burden, but also targeting SphK1 with a specific inhibitor reduced tumor growth, lymph node and lung metastasis, and decreased hem- and lymphangiogenesis around the primary tumor and in the lymph nodes. Our results suggest that targeting SphK1 and S1P may be a useful additional modality for treatment of metastatic breast cancer.

Materials and Methods

Cell culture

4T1-luc2 cells, a mouse mammary fat pad-derived adenocarcinoma cell line that has been engineered to express luciferase (Caliper Life Sciences), were cultured in RPMI Medium 1640 with 10% fetal bovine serum. GFP-expressing human umbilical vein endothelial cells (HUVECs) and GFP-expressing human lymphatic endothelial cells (HLECs) purchased from Angio-Proteomie were maintained in endothelial cell medium supplemented with 5% FBS and endothelial cell growth supplement (ScienCell).

Construction of lentiviral shRNAs for mouse SphK1

Three sense sequences of siRNA cassettes specifically targeting the nucleotides of mouse SphK1 (Accession number: NM_011451.1) were designed using siRNA Target Finder (Ambion). The specificity of the selected sequences was confirmed by BLAST search. The lentiviral shRNAs were constructed using a pLL3.7 expression vector as described previously (24). The sequences of the shRNAs for mouse SphK1 are as following: shRNA 1, 5'- GCACCCAAACTACCTTTGGAT-3'; shRNA 2, 5'-GCACCTTCTTTCGCCTAGCAA-3'; shRNA 3, 5'-GAGGCAGAGATAACCTTTAAA-3'. Recombinant lentivirus was produced by cotransfection of 293FT cells with lentiviral vector and the packaging vectors using calcium phosphate. The viruses were collected from the culture medium and purified by polyethyleneglycol precipitation. The transduction efficiency of lentivirus in 4T1 cells was determined by fluorescence microscopy. The silencing efficiency was determined using quantitative PCR (qPCR) and western blot analysis.

Syngeneic tumor model

All animal studies were conducted in the Animal Research Core Facility at VCU School of Medicine in accordance with the institutional guidelines. All procedures were approved by the VCU Institutional Animal Care and Use Committee (IACUC) that is accredited by Association for Assessment and Accreditation of Laboratory Animal Care (AAALAC). Female BALB/c mice, 8 to12 weeks of age, weighing approximately 20g were obtained from Harlan. 4T1-luc2 cells (1×10^5 cells in 10μl RPMI) were surgically implanted in the upper fat pads under direct vision. One day after implantation, mice were randomized by tumor size determined by bioluminescence with the IVIS Imaging System (Xenogen). SK1-I in PBS was injected intraperitoneally, as indicated, every day at a dose of 20 mg/kg. At the indicated times, the animals were sacrificed by exsanguination, blood was collected, tumors excised, weighed, fixed in formalin and embedded in paraffin or frozen in liquid nitrogen.

Bioluminescent quantification of tumor burden

D-luciferin (0.2ml of 15mg/ml stock, Caliper Life Sciences) was injected intraperitoneally into mice previously implanted with 4T1-luc2 cells. Living Image Software (Xenogen) was used to quantify the photons/sec emitted by the cells. Bioluminescence was measured and quantified at five min intervals over thirty min using a subject height of 1.5 cm, medium binning and an exposure time of 0.5 sec to 1 min. Bioluminescence was then determined by the peak number of photons/sec calculated over this time frame. Axillary lymph node metastasis was quantified *in vivo* after intraperitoneal injection of luciferin and primary tumor resection. Lung metastasis was quantified *ex vivo* after the lungs were removed.

Quantification of sphingolipids by mass spectrometry

Lipids were extracted from serum and tissues and sphingolipids quantified by liquid chromatography, electrospray ionization-tandem mass spectrometry (LC-ESI-MS/MS, 4000 QTRAP, AB Sciex) as described (25).

Directed in vivo angiogenesis assays (DIVAA) and cell isolation

Angioreactors (DIVAA kit, Invitrogen) were implanted into the subcutaneous layer of the back of 8 week-old nude mice under anesthesia according to the manufacturer's instructions. Mice were euthanized with CO_2 at day 11 after implantation and the angioreactors were removed under stereomicroscopy (SZ51, Olympus).

Fluorescence activated cell sorting (FACS)

Single-cell suspensions were obtained from lymph nodes as described (26). For DIVAA/FACS analyses, Matrigel and fibrotic reactive tissue in the open end of the angioreactors were removed with DMEM and digested with a mixture of 9 ml of Cell Sparse (Invitrogen) containing 0.1% collagenase type 2 (GIBCO), 1 ml of 0.25 U/ml dispase (GIBCO), and 75 μl of 0.1% DNase (Invitrogen) for 30 min to obtain single-cell suspensions. Tumors were minced and digested similarly. Cell suspensions were blocked with anti-CD16/CD32 (Mouse BD Fc Block, BD Biosciences) and then stained with the following antibodies as indicated: Alexa 488-conjugated lyve1 (eBioscience); PE-conjugated podoplanin, PerCP-Cy5.5-conjugated CD45, APC-conjugated CD31, Alexa 700-conjugated TER-119 (Biolegend); or appropriate matched, fluorochrome-labeled isotype control monoclonal antibody (mAb). The LIVE/DEAD Viability Assay kit (Invitrogen) was used to eliminate dead cells. Cells were analyzed by FACS using BD FACSCanto II and BD FACSAria II (BD Biosciences), and corollary data assessed with BD FACSDiva Software version 6.1.3 (BD Biosciences).

Histopathological analysis and vessel density determination

Immediately after sacrifice of the animals, tumor samples were fixed in 10% neutral buffered formalin for immunohistochemical analyses of cell proliferation and apoptosis. 4T1-luc2 cell proliferation in the tumor was determined by staining histological sections with monoclonal antibodies against Ki-67 (Dako), a nuclear protein expressed in proliferating cells. Apoptosis was determined by terminal uridine deoxynucleotidyl transferase dUTP nick end labelling (TUNEL) assay using the ApopTag Peroxidase In Situ Apoptosis Detection Kit S7100 (Millipore).

The tumors were also frozen, and embedded in optimal cutting medium (OCT 4583, Sakura Finetek) for immunofluorescent analysis for hem- and lymphangiogenesis. The sections were stained with the following antibodies as indicated: CD31 (BD), LYVE-1 (abcam) and F4/80 (kindly provided by Bin-Zhi Qian in Jeffrey Pollard laboratory at Albert Einstein College of Medicine (27)).The stained sections of were examined with LSM510 laser-scanning confocal microscopes (Zeiss) and microvessel density was determined as previously described (28).

Patient samples

All studies using patient samples were conducted accordance with the institutional guidelines after approval by VCU Institutional Review Board. Human sera were collected by the Tissue and Data Acquisition and Analysis Core of VCU and S1P levels determined in serum from Stage IIIA breast cancer patients and age/ethnicity matched healthy volunteers.

In vitro assays

Cell number of 4T1-luc2 cells was determined by measurement of luciferase activity with luciferin substrate (Caliper Life Sciences) using a VICTOR X4 Multilabel Plate Reader (PerkinElmer). qPCR (15), and tube formation assay were conducted as described previously (29),

Statistical analysis

Results were analyzed for statistical significance with a two-tailed Student's t-test, with $p < 0.05$ considered significant. Experiments were repeated at least three times in triplicate with consistent results. *In vivo* experiments were repeated three times and each experimental group consisted of at least six mice.

Results

Up-regulation of SphK1 and increased S1P levels in 4T1-luc2 tumor progression

Previous studies showed that S1P and SphK1, the enzyme that produces it, regulate many processes important for breast cancer (15). To examine their involvement in breast cancer progression *in vivo*, we utilized an enhanced syngeneic mouse metastatic breast cancer model in which 4T1-luc2 murine breast cancer cells were orthotopically implanted under direct vision into the chest mammary fat pads of immune-competent mice. We have found that this chest orthotopic model more accurately mimics human breast cancer progression than subcutaneous models. Indeed, 4T1-luc2 cells produced large tumors in the chest mammary fat pad that rapidly metastasized and increased total tumor burden (Fig. 1A). Metastatic spread to the regional axillary lymph nodes and the lungs was quantified by bioluminescence after removal of the 4T1-luc2 tumors from the implantation sites (primary tumors). As can be seen in Fig. 1B, lymph node metastases emerged earlier than lung metastases, with a rapid increase in incidence of metastasis to the lymph nodes, similar to common human breast cancer progression.

Expression of both SphK1 and SphK2 is very low in naïve mammary fat pads, whereas 4T1-luc2 cells express much higher levels of SphK1 mRNA than SphK2 (Fig. 1C). However, after implantation in mammary fat pads, SphK1 mRNA levels in breast tumors were significantly increased (Fig. 1C), with concomitantly increased S1P levels in the tumors (Fig. 2E). Interestingly, levels of S1P in serum from these mice were also significantly elevated (Fig. 1D), suggesting that overexpression of SphK1 in the tumors may be responsible for the increased circulating S1P.

Since it has been shown that overexpression of SphK1 correlates with poor prognosis of breast cancer patients (20), it was of interest to measure serum levels of S1P in breast cancer patients. We found that the serum S1P levels were significantly elevated in stage IIIA breast cancer patients who have lymph node metastases, compared to age/ethnicity-matched healthy volunteers (Fig. 1E).

Growth of primary mammary tumors, tumor burden, and lymph node and lung metastases are reduced by inhibition of SphK1

We next examined the effect of inhibition of SphK1 with SK1-I ((2R,3S,4E)-N-methyl-5-(4-pentylphenyl)-2-aminopent-4-ene-1,3-diol (BML-258)) (30). SKI-I is a potent, water-soluble, isoenzyme-specific inhibitor of SphK1, that in contrast to pan-SphK inhibitors, does not inhibit SphK2, protein kinase C, or numerous other protein kinases (30). Consistent with previous studies in other types of cancer cells (30, 31), SK1-I inhibited growth of 4T1-luc2 cells in a dose-dependent manner (Fig. 2A). A significant effect was observed at a concentration of 3 μM and complete inhibition of growth at 10 μM (Fig. 2A). We confirmed

that SK1-I decreased the enzyme activity of SphK1 and that down-regulation of SphK1 with specific siRNA, similar to SK1-I, also suppressed growth of these cells (data not shown). We first examined circulating levels of SK1-I following a single intraperitoneal injection of 20 mg/kg. Plasma SK1-I levels reached a maximum concentration of 0.6 μM within 2 hours but still could be detected up to 12 hours. Concomitantly, plasma levels of S1P were significantly reduced up to 12 hours (Supplementary Fig. S1). We then investigated the effect of SK1-I on growth of 4T1-luc2 tumors in mouse mammary fat pads. Intraperitoneal injections of SK1-I significantly reduced both tumor volume and weight (Fig. 2B, C). The tumors from animals treated with SK1-I also showed reduced mitotic activity compared to those from vehicle treated animals as demonstrated by Ki67 immunohistochemistry (Fig. 2D). Conversely, TUNEL staining revealed a large increase in apoptotic cells in tumors from SK1-I treated mice (Fig. 2D). Consistent with the up-regulation of SphK1 in tumor (Fig. 1C), S1P levels in tumors gradually increased compared to naïve or sham operated mammary fat pads as measured by LC-ESI-MS/MS. This rise of S1P in the tumors was prevented by treatment with SK1-I (Fig. 2E). Notably, SK1-I was taken up by the mammary tumors and its levels gradually increased with time (Fig. 2F).

The total tumor burden determined by the IVIS Imaging System was also significantly suppressed by SK1-I treatment (Fig. 3A). Serum S1P levels, which are elevated in the tumor bearing mice, were also reduced by SK1-I treatment (Fig. 3B). Serum levels of SK1-I in these mice increased with time (Fig. 3C). Importantly, SK1-I significantly reduced lymph node and lung metastases (Fig. 3D, E). Taken together, these results suggest that S1P produced by SphK1 in the mammary tumors is involved in lymph node and lung metastasis.

SK1-I suppresses *in vitro* hemangiogenesis and lymphangiogenesis

Because hem- and lymphangiogenesis are considered to play critical roles in lymph node and lung metastasis (28), it was of interest to next examine the role of S1P generated by SphK1 in these processes. We first determined the effect of S1P on *in vitro* hem- and lymphangiogenesis. In agreement with previous studies (22, 32), we found that S1P is a potent hem- and lymphangiogenic factor for human blood and lymphatic endothelial cells, respectively, as demonstrated by enhanced tube formation (Fig. 4A, B), which reflects cell migration and organization of a network architecture, key aspects of both hem- and lymphangiogenesis. Angiopoietin 2 (Ang2), whose levels in breast cancer correlate with metastases to lymph nodes and poor prognosis (33), was used as a positive control. SK1-I inhibited *in vitro* hem- and lymphangiogenesis (Fig. 4A, B), suggesting that the effects of Ang2 are mediated at least in part by SphK1 and formation of S1P.

We next sought to determine whether high expression of SphK1 and S1P production in 4 T 1-luc2 cells contribute to enhanced lymphangiogenesis and hemangiogenesis. Whereas supernatants from 4T1-luc2 cells significantly stimulate tube formation of HUVECs and HLECs, shRNA knockdown of SphK1, which decreased SphK1 expression (Supplementary Fig. S2A, B) and release of S1P (Supplementary Fig. S2C) markedly reduced them (Supplementary Fig. S2D, E). Moreover, treatment with S1P did not affect expression of either VEGF-A or VEGF-C mRNA in 4T1-luc2 cells (Supplementary Fig. S3). These results indicate that S1P produced by SphK1 in 4T1-luc2 breast cancer cells is an important contributor to hem- and lymphangiogenesis.

Involvement of SphK1 and S1P in *in vivo* hemangiogenesis and lymphangiogenesis

Directed in vivo angiogenesis assays (DIVAA) provide a simple and quantitative method to measure hemangiogenesis *in vivo* (34). In contrast, one of the challenges of studying lymphangiogenesis *in vivo* is the lack of assays for objective quantification (12). To this end, we developed a similar approach to simultaneously quantify both hem- and

lymphangiogenesis by combining DIVAA with fluorescence activated cell sorting (DIVAA/FACS).

We initially modified the FACS gating scheme established by Pham et al (23) to separate lymph node blood endothelial cells (BECs) and lymphatic endothelial cells (LECs) from other cells. TER-119 and CD45 were used to gate out red blood cells and leukocytes, respectively (Fig. 5A). LECs and BECs were quantified using gp38 (podoplanin) and lymphatic vessel endothelial hyaluronan receptor (LYVE-1), specific markers for LECs, and CD31, a specific marker for both BECs and LECs. LECs were identified as $CD45^{-}CD31^{+}gp38^{-}$, BECs as $CD45^{-}CD31\ gp38^{-}$, and fibroblast reticular cells (FRCs) as $CD45^{-}CD31^{-}gp38^{+}$. As expected, the selected population of LECs showed higher expression of LYVE-1 than BECs or FRCs (Fig. 5B).

In the DIVAA approach, mice are implanted subcutaneously with silicone cylinders (angioreactors) that are closed at one end and filled with 20 μl of Matrigel (34). The addition of stimuli enables directional migration of BECs and LECs into the angioreactors, which proliferate and form appropriate vessels. In agreement with previous studies (34), hemangiogenesis was readily observable by the appearance of blood vessels (Fig. 5C). Both S1P and Ang2 significantly induced hemangiogenesis 11 days after implantation of the angioreactors (Fig. 5C). To simultaneously quantify hem-and lymphangiogenesis, cells were isolated from the angioreactors by collagenase digestion, followed by FACS analysis to separate the BECs from LECs and other cells as described above. Interestingly, both S1P and Ang2 enhanced the migration of BECs and LECs into the angioreactors, although hemangiogenesis was more pronounced than lymphangiogenesis (Fig. 5D, E). Similar to its effect on *in vitro* hem- and lymphangiogenesis (Fig. 4B), the inclusion of SK1-I in the angioreactors together with Ang2 completely abolished its ability to stimulate both of these processes (Fig. 5E).

Inhibition of SphK1 suppresses hemangiogenesis and lymphangiogenesis in tumors and in lymph nodes *in vivo*

To establish that S1P generated by SphK1 plays a critical role in tumor-induced hem- and lymphangiogenesis *in vivo*, we next examined the effect of SK1-I on hem- and lymphangiogenesis in the tumors themselves and in the draining lymph nodes. FACS analysis of mammary pad tumors revealed that both BECs and LECs were greatly reduced by treatment of mice with SK1-I (Fig. 6A, B). Interestingly, the number of BECs and LECs in lymph nodes, the host tumor microenvironment, was significantly increased in tumor-bearing animals compared to sham animals and treatment with SK1-I inhibited the increase of both BECs and LECs in lymph nodes (Fig. 6C, D). Morphometric analysis confirmed that SK1-I reduced both tumor-induced hem- and lymphangiogenesis as determined by densities of $CD31^{+}$ LYVE-1^{-} blood vessels (BVD) and $CD31^{+}$LYVE-1^{+} lymphatic vessels (LVD), respectively (Fig. 6E, F).

Discussion

Previous studies have shown that SphK1 is overexpressed in breast cancer and its level of expression correlates with resistance to treatments and poor patient outcomes (16, 18, 20). However, several factors have hindered progress in determining the role of S1P, the product of SphK1, in tumorigenesis and tumor-induced hem- and lymphangiogenesis *in vivo*. First, since S1P has such a profound role in immune function (35), studies of traditional *in vivo* metastatic breast cancer models with xenografts in immune compromised mice that ignore the host immune response to cancer may be difficult to interpret. Second, it has not been possible to accurately quantify S1P in tumors until recently with the development of high sensitivity mass spectrometric assays (25). To this end, we utilized our newly established

syngeneic breast cancer model, which not only retains the host immune responses but also more closely models progression of the human disease by forming lymph node and lung metastasis leading to metastatic spread and death. Our data indicates that SphK1 is the predominant isoenzyme expressed in 4T1-luc2 cells and is further up-regulated in tumors, in contrast to SphK2. This is in agreement with previous reports correlating expression of SphK1 but not of SphK2 with poor prognosis in breast cancer (20). We found that levels of S1P gradually increased both in tumors and in serum determined by LC-ESI-MS/MS and correlated with tumor burden. Moreover, treatment of tumor bearing animals with the specific SphK1 inhibitor SK1-I reduced S1P levels in the tumor and in circulation, and greatly reduced the size of the primary tumor, lymph node and lung metastasis. This is in agreement with a previous report that blood and tumor S1P levels were increased in mice with colon cancer (36).

Quantification of tumor-induced hem- and lymphangiogenesis has remained a challenge (12). This is usually examined by histological determinations of microvessel density or lymphatic vessel density, which rely on selective morphometric analysis (e.g. vessel counts, vascular morphology, etc.) (12). The strengths of the morphological approach are that it can evaluate the location of the vessels in relationship to the tumor and identify/quantify morphological changes that lymphatic vessels undergo during tumor progression. The limitations include variable sites of tissue sectioning, variable immunostaining techniques, different vessel density quantification methods, and the lack of standardization in the estimation of hem- and lymphangiogenesis (12). To compliment this approach and overcome some of these limitations, we developed a flow cytometry method to quantify both BECs and LECs in the same sample to simultaneously evaluate both hem- and lymphangiogenesis. Flow cytometric analysis can provide supportive data to quantify the changes in BECs and LECs.

Consistent with both the *in vitro* tube formation and DIVAA/FACS assays, we demonstrated that exogenous S1P enhanced hem- and lymphangiogenesis. In this regard, Anelli et al showed that down-regulation of SphK1 did not change the levels of VEGF-A or VEGF-C secretion in glioma cells, and down-regulation of SphK1, but not VEGF-A or VEGF-C, suppressed glioma-induced hemangiogenesis (37). Utilizing shSphK1, we confirmed that tumor-derived S1P mediates tumor-induced hem- and lymphangiogenesis without altering VEGF-A or VEGF-C (Supplementary Fig. S3), which is in agreement with Anelli et al (37). Taken together, S1P is an important stimulator of hem- and lymphangiogenesis *in vitro*.

SK1-I decreased hem- and lymphangiogenesis not only around the primary tumor, but also in lymph nodes that are distant from the tumor. Further, we have observed by F4/80 immunofluorescent staining of that SK1-I also reduced macrophage recruitment surrounding the tumor (Supplementary Fig. S4). Macrophages are cellular components of the tumor microenvironment that promote hem- and lymphangiogenesis (38, 39). Thus, in addition to direct effects on hem- and lymphangiogenesis, S1P can indirectly affect the tumor microenvironment to further enhance these processes.

In sum, S1P generated by SphK1 is important not only for tumor progression but also for tumor-induced hemangiogenesis and lymphangiogenesis and therefore targeting SphK1 and its product S1P would be a multi-pronged attack against breast cancer.

Supplementary Material

Refer to Web version on PubMed Central for supplementary material.

Acknowledgments

We thank the Tissue and Data Acquisition and Analysis Core (TDAAC) of VCU for collection of human samples, and the Anatomic Pathology Research Services (APRS) Director, Dr. Jorge A. Almenara, and the histotechnologists for technical assistance with tissue processing, sectioning and staining. The Flow Cytometry and Confocal microscopy Shared Resource Cores were supported in part by NIH Grant P30CA16059 to the Massey Cancer Center and NINDS Center core Grant 5P30NS047463, respectively.

Grant Support

This work was supported by NCI grant R01CA61774 to SS and NIH grant K12HD055881 and Susan G. Komen for the Cure Research Foundation Career Catalyst Research Grant KG090510 to KT. MN was supported by the SUMITOMO Life Social Welfare Services Foundation.

References

1. Siegel R, Ward E, Brawley O, Jemal A. Cancer statistics: 2011: the impact of eliminating socioeconomic and racial disparities on premature cancer deaths. CA Cancer J Clin. 2011; 61:212–236. [PubMed: 21685461]
2. Mumprecht V, Honer M, Vigl B, Proulx ST, Trachsel E, Kaspar M, et al. In vivo imaging of inflammation- and tumor-induced lymph node lymphangiogenesis by immuno-positron emission tomography. Cancer Res. 2010; 70:8842–8851. [PubMed: 20978206]
3. Hanahan D, Weinberg RA. Hallmarks of cancer: the next generation. Cell. 2011; 144:646–674. [PubMed: 21376230]
4. Nagahashi M, Shirai Y, Wakai T, Sakata J, Ajioka Y, Nomura T, et al. Depth of invasion determines the postresectional prognosis for patients with T1 extrahepatic cholangiocarcinoma. Cancer. 2010
5. Folkman J. Tumor angiogenesis: therapeutic implications. N Engl J Med. 1971; 285:1182–1186. [PubMed: 4938153]
6. Holmgren L, O'Reilly MS, Folkman J. Dormancy of micrometastases: balanced proliferation and apoptosis in the presence of angiogenesis suppression. Nat Med. 1995; 1:149–153. [PubMed: 7585012]
7. Hanahan D, Weinberg RA. The hallmarks of cancer. Cell. 2000; 100:57–70. [PubMed: 10647931]
8. Miller K, Wang M, Gralow J, Dickler M, Cobleigh M, Perez EA, et al. Paclitaxel plus bevacizumab versus paclitaxel alone for metastatic breast cancer. N Engl J Med. 2007; 357:2666–2676. [PubMed: 18160686]
9. Miles DW, Chan A, Dirix LY, Cortes J, Pivot X, Tomczak P, et al. Phase III study of bevacizumab plus docetaxel compared with placebo plus docetaxel for the first-line treatment of human epidermal growth factor receptor 2-negative metastatic breast cancer. J Clin Oncol. 2010; 28:3239–3247. [PubMed: 20498403]
10. Robert NJ, Dieras V, Glaspy J, Brufsky AM, Bondarenko I, Lipatov ON, et al. RIBBON-1: randomized, double-blind, placebo-controlled, phase III trial of chemotherapy with or without bevacizumab for first-line treatment of human epidermal growth factor receptor 2-negative, locally recurrent or metastatic breast cancer. J Clin Oncol. 2011; 29:1252–1260. [PubMed: 21383283]
11. Edge, SB.; Byrd, DR.; Compton, CC.; Fritz, AG.; Greene, FL.; Trotti, A., et al. AJCC cancer staging manual. 7th ed. New York, NY: Springer; 2010.
12. Nagahashi M, Ramachandran S, Rashid OM, Takabe K. Lymphangiogenesis: a new player in cancer progression. World J Gastroenterol. 2010; 16:4003–4012. [PubMed: 20731013]
13. Tammela T, Alitalo K. Lymphangiogenesis: Molecular mechanisms and future promise. Cell. 2010; 140:460–476. [PubMed: 20178740]
14. Cueni LN, Hegyi I, Shin JW, Albinger-Hegyi A, Gruber S, Kunstfeld R, et al. Tumor lymphangiogenesis and metastasis to lymph nodes induced by cancer cell expression of podoplanin. Am J Pathol. 2010; 177:1004–1016. [PubMed: 20616339]
15. Takabe K, Paugh SW, Milstien S, Spiegel S. "Inside-out" signaling of sphingosine-1-phosphate: therapeutic targets. Pharmacol Rev. 2008; 60:181–195. [PubMed: 18552276]
16. Pyne NJ, Pyne S. Sphingosine 1-phosphate and cancer. Nat Rev Cancer. 2010; 10:489–503. [PubMed: 20555359]

17. Takabe K, Kim RH, Allegood JC, Mitra P, Ramachandran S, Nagahashi M, et al. Estradiol induces export of sphingosine 1-phosphate from breast cancer cells via ABCC1 and ABCG2. J Biol Chem. 2010; 285:10477–10486. [PubMed: 20110355]
18. Shida D, Takabe K, Kapitonov D, Milstien S, Spiegel S. Targeting SphK1 as a new strategy against cancer. Curr Drug Targets. 2008; 9:662–673. [PubMed: 18691013]
19. Kim RH, Takabe K, Milstien S, Spiegel S. Export and functions of sphingosine-1-phosphate. Biochim Biophys Acta. 2009; 1791:692–696. [PubMed: 19268560]
20. Ruckhaberle E, Rody A, Engels K, Gaetje R, von Minckwitz G, Schiffmann S, et al. Microarray analysis of altered sphingolipid metabolism reveals prognostic significance of sphingosine kinase 1 in breast cancer. Breast Cancer Res Treat. 2008; 112:41–52. [PubMed: 18058224]
21. Milstien S, Spiegel S. Targeting sphingosine-1-phosphate: a novel avenue for cancer therapeutics. Cancer Cell. 2006; 9:148–150. [PubMed: 16530698]
22. Yoon CM, Hong BS, Moon HG, Lim S, Suh PG, Kim YK, et al. Sphingosine-1-phosphate promotes lymphangiogenesis by stimulating S1P1/Gi/PLC/Ca2+ signaling pathways. Blood. 2008; 112:1129–1138. [PubMed: 18541717]
23. Pham TH, Baluk P, Xu Y, Grigorova I, Bankovich AJ, Pappu R, et al. Lymphatic endothelial cell sphingosine kinase activity is required for lymphocyte egress and lymphatic patterning. J Exp Med. 2010; 207:17–27. S1-S4. [PubMed: 20026661]
24. Zhou H, Jarujaron S, Gurley EC, Chen L, Ding H, Studer E, et al. HIV protease inhibitors increase TNF-alpha and IL-6 expression in macrophages: involvement of the RNA-binding protein HuR. Atherosclerosis. 2007; 195:e134–e143. [PubMed: 17531241]
25. Hait NC, Allegood J, Maceyka M, Strub GM, Harikumar KB, Singh SK, et al. Regulation of histone acetylation in the nucleus by sphingosine-1-phosphate. Science. 2009; 325:1254–1257. [PubMed: 19729656]
26. van Beijnum JR, Rousch M, Castermans K, van der Linden E, Griffioen AW. Isolation of endothelial cells from fresh tissues. Nat Protoc. 2008; 3:1085–1091. [PubMed: 18546599]
27. Qian BZ, Li J, Zhang H, Kitamura T, Zhang J, Campion LR, et al. CCL2 recruits inflammatory monocytes to facilitate breast-tumour metastasis. Nature. 2011; 475:222–225. [PubMed: 21654748]
28. Nagahashi M, Shirai Y, Wakai T, Sakata J, Ajioka Y, Hatakeyama K. Perimuscular connective tissue contains more and larger lymphatic vessels than the shallower layers in human gallbladders. World J Gastroenterol. 2007; 13:4480–4483. [PubMed: 17724804]
29. Wang F, Van Brocklyn JR, Hobson JP, Movafagh S, Zukowska-Grojec Z, Milstien S, et al. Sphingosine 1-phosphate stimulates cell migration through a G(i)- coupled cell surface receptor. Potential involvement in angiogenesis. J Biol Chem. 1999; 274:35343–35350. [PubMed: 10585401]
30. Paugh SW, Paugh BS, Rahmani M, Kapitonov D, Almenara JA, Kordula T, et al. A selective sphingosine kinase 1 inhibitor integrates multiple molecular therapeutic targets in human leukemia. Blood. 2008; 112:1382–1391. [PubMed: 18511810]
31. Kapitonov D, Allegood JC, Mitchell C, Hait NC, Almenara JA, Adams JK, et al. Targeting sphingosine kinase 1 inhibits Akt signaling, induces apoptosis, and suppresses growth of human glioblastoma cells and xenografts. Cancer Res. 2009; 69:6915–6923. [PubMed: 19723667]
32. Lee MJ, Thangada S, Claffey KP, Ancellin N, Liu CH, Kluk M, et al. Vascular endothelial cell adherens junction assembly and morphogenesis induced by sphingosine-1-phosphate. Cell. 1999; 99:301–312. [PubMed: 10555146]
33. Sfiligoi C, de Luca A, Cascone I, Sorbello V, Fuso L, Ponzone R, et al. Angiopoietin-2 expression in breast cancer correlates with lymph node invasion and short survival. Int J Cancer. 2003; 103:466–474. [PubMed: 12478661]
34. Guedez L, Rivera AM, Salloum R, Miller ML, Diegmueller JJ, Bungay PM, et al. Quantitative assessment of angiogenic responses by the directed in vivo angiogenesis assay. Am J Pathol. 2003; 162:1431–1439. [PubMed: 12707026]
35. Spiegel S, Milstien S. The outs and the ins of sphingosine-1-phosphate in immunity. Nat Rev Immunol. 2011; 11:403–415. [PubMed: 21546914]

36. Kawamori T, Kaneshiro T, Okumura M, Maalouf S, Uflacker A, Bielawski J, et al. Role for sphingosine kinase 1 in colon carcinogenesis. FASEB J. 2009; 23:405–414. [PubMed: 18824518]
37. Anelli V, Gault CR, Snider AJ, Obeid LM. Role of sphingosine kinase-1 in paracrine/transcellular angiogenesis and lymphangiogenesis in vitro. FASEB J. 2010
38. Qian BZ, Pollard JW. Macrophage diversity enhances tumor progression and metastasis. Cell. 2010; 141:39–51. [PubMed: 20371344]
39. Ji RC. Macrophages are important mediators of either tumor- or inflammation-induced lymphangiogenesis. Cell Mol Life Sci. 2011

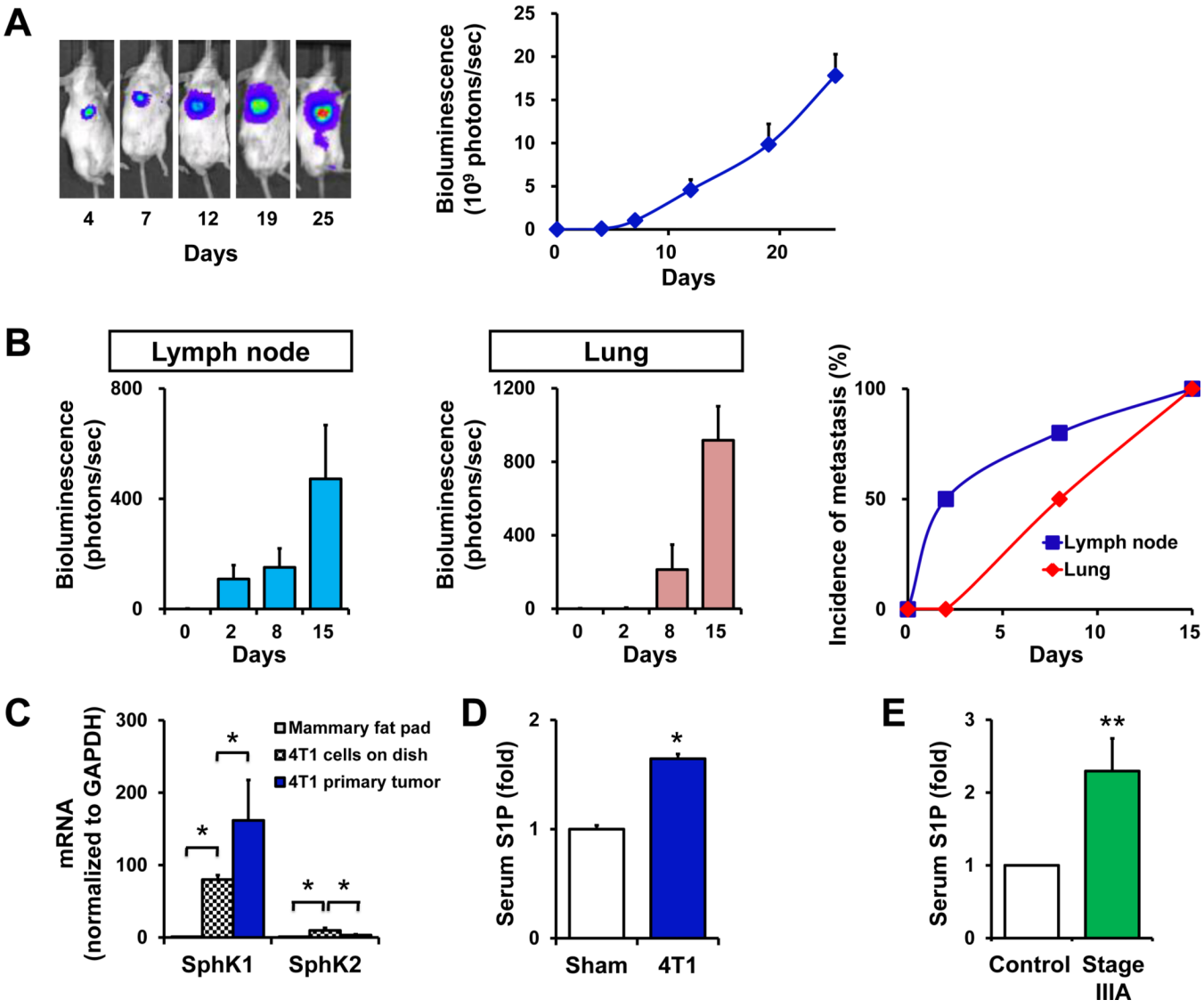

Figure 1. The SphK1/S1P axis in breast cancer progression

(A) 4T1 breast tumors were established by surgical implantation of 4T1-luc2 cells into the chest mammary fat pad under direct vision. The tumor burden was determined by bioluminescence technology. Representative IVIS images (left) and bioluminescent quantification (right) on the indicated days are shown. (B) Axillary lymph node metastases were measured by bioluminescence at the indicated times when breast tumor was removed for accurate measurement (left). Lung metastases were measured separately *ex vivo* (middle). The incidences of metastases to the axillary lymph nodes and the lung were determined on the indicated days (right). (C) mRNA was isolated from mammary fat pads of naïve BALB/c mice (gray filled bars), cultured 4T1-luc2 cells (black cross hatched bars), and primary tumors in the chest mammary fat pads formed by 4T1-luc2 cells (blue filled bars) 10 days after implantation. Expression of SphK1 and SphK2 was determined by QPCR and normalized to levels of GAPDH mRNA. Data are expressed as fold increases ± S.D. (D) S1P levels were determined by LC-ESI-MS/MS in the serum of sham surgery mice and in mice with 4T1-luc2 xenograft tumors 15 days after implantation. Data are expressed as fold increases ± SEM. (E) S1P was measured in serum from stage IIIA breast cancer patients and age/ethnicity-matched healthy volunteers (n = 5). *, $P < 0.001$; **, $P < 0.05$.

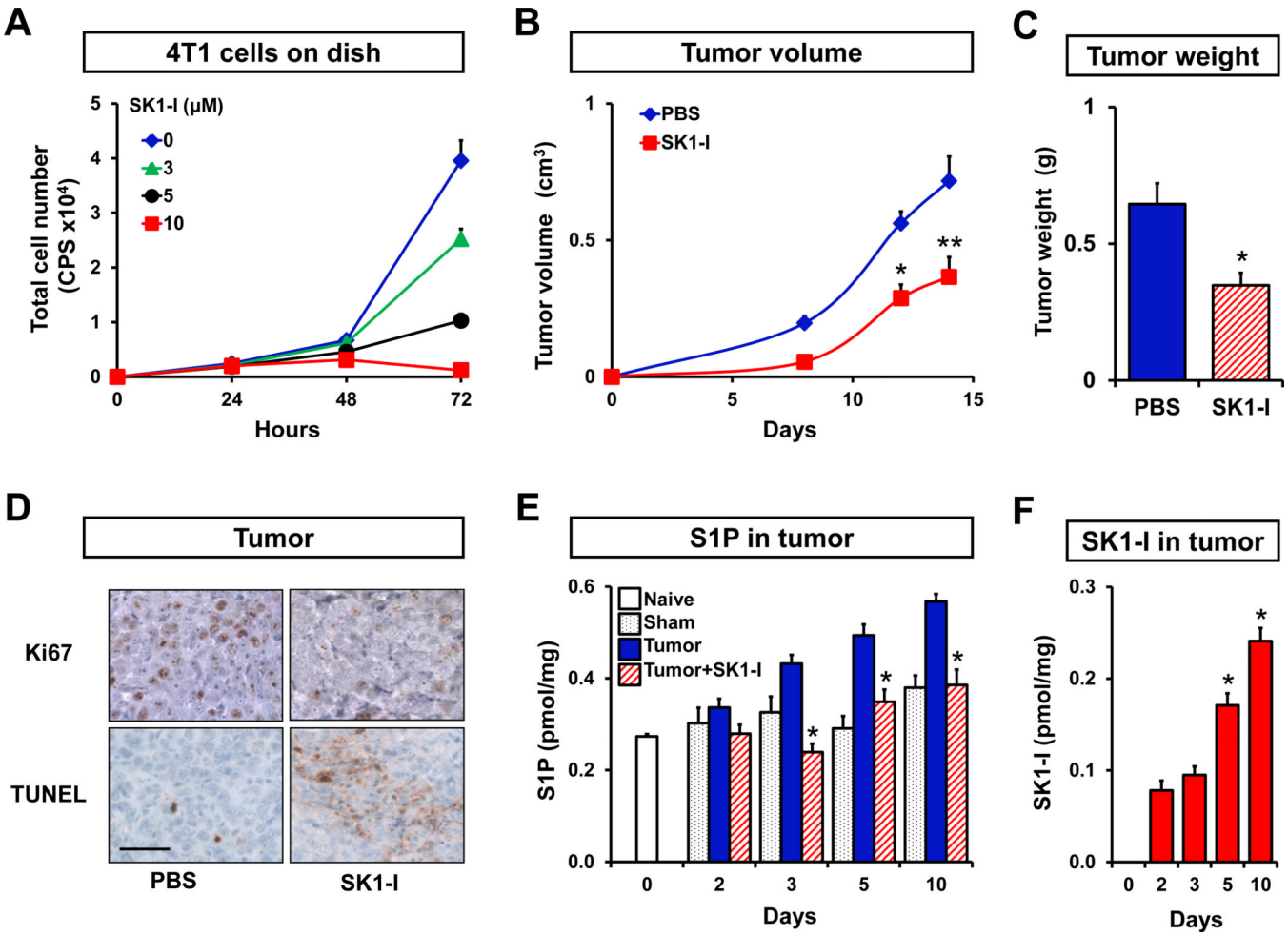

Figure 2. Inhibition of SphK1 decreases growth of 4T1-luc2 mammary tumors

(A) 4T1-luc2 cells were treated with the indicated concentration of SK1-I and total cell number was determined by measurement of luciferase activity. 4T1-luc2 cells were surgically implanted in mammary fat pads under direct vision. Tumor-bearing mice were randomized into two groups and injected i.p. with PBS or SK1-I (20 mg/kg) daily. Tumor volumes were measured on the indicated days (B) and tumor weights were determined after excision on day 18 (C) (n = 5 per group). (D) Tumor histology. Paraffin-embedded tumor sections were immunostained with Ki67 and counterstained with hematoxylin. Apoptotic cells were visualized by TUNEL staining. Scale bar, 50 μm. (E) S1P levels were determined by LC-ESI-MS/MS in mammary fat pads of naïve (open bar) and sham operated mice (black dotted bars), and in mammary tumors from mice that were treated with PBS (blue filled bars) or SK1-I (red hatched bars) on the indicated days. (F) SK1-I levels were determined on the indicated days by LC-ESI-MS/MS in mammary tumors from mice that were treated with SK1-I (red filled bars), and means ± SEM are shown. *, $P < 0.01$; **, $P < 0.05$.

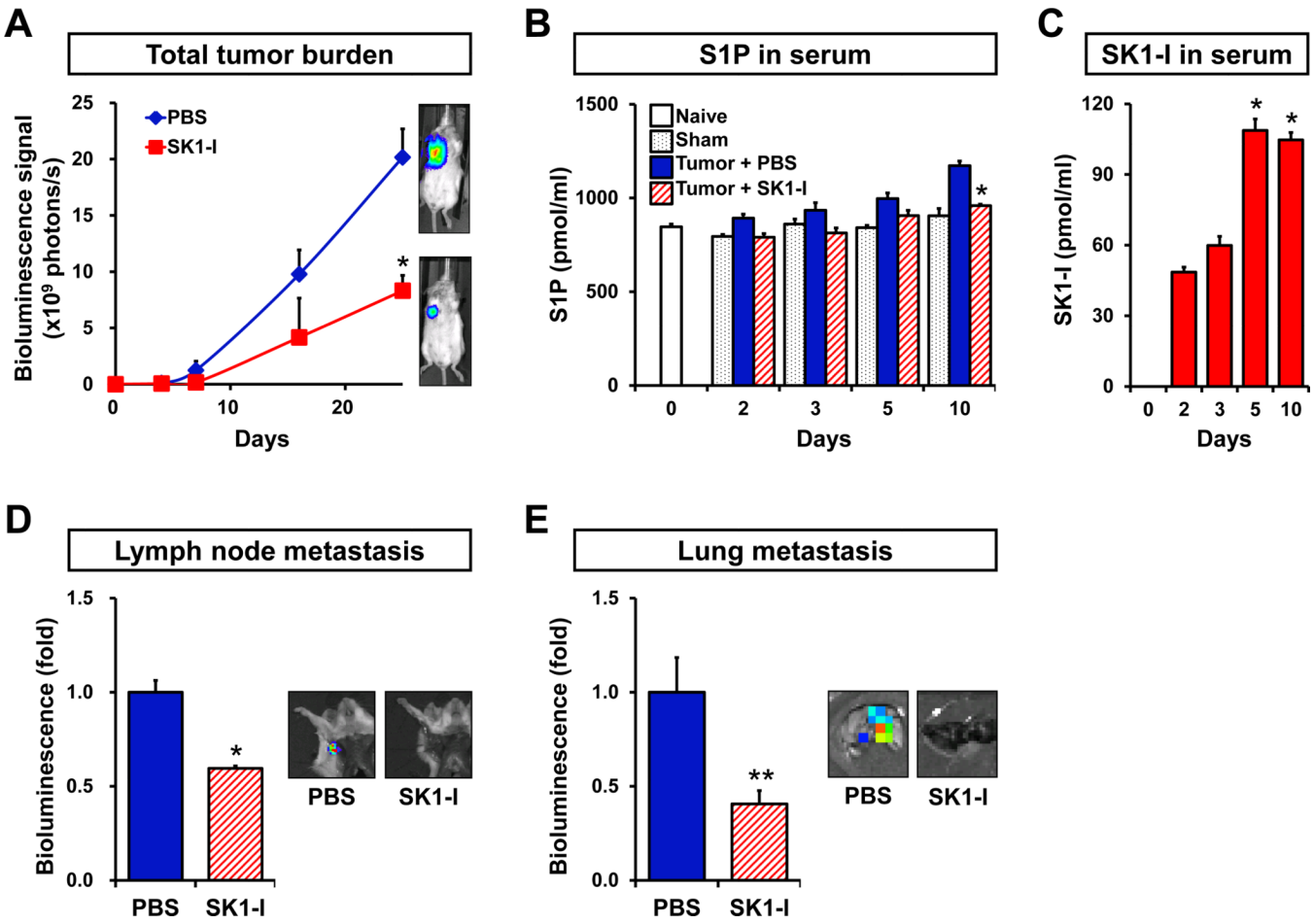

Figure 3. SK1-I decreases tumor burden, lymph node and lung metastases, and circulating levels of S1P

4T1-luc2 cells were surgically implanted in mammary fat pads under direct vision. Tumor-bearing mice were randomized into two groups and injected i.p. daily with PBS or SK1-I (20 mg/kg) (n = 5). (A) Tumor burden was quantified by *in vivo* bioluminescence on the indicated days. Right panels show representative IVIS bioluminescent images. (B) S1P levels were determined by LC-ESI-MS/MS in serum of naïve (open bar) and sham operated mice (black dotted bars), mice bearing 4T1-luc2 tumors that were treated with PBS (blue filled bars) or SK1-I (red hatched bars) on the indicated days. (C) SK1-I levels were determined on the indicated days by LC-ESI-MS/MS in serum from the mice that were treated with SK1-I (red filled bars). Representative bioluminescent images (right) and quantification of regional lymph node (D) and lung (E) metastases were determined by bioluminescence 7 or 10 days after treatment with PBS or SK1-I, respectively. Data are expressed as mean ± SEM. *, $P < 0.01$; **, $P < 0.05$.

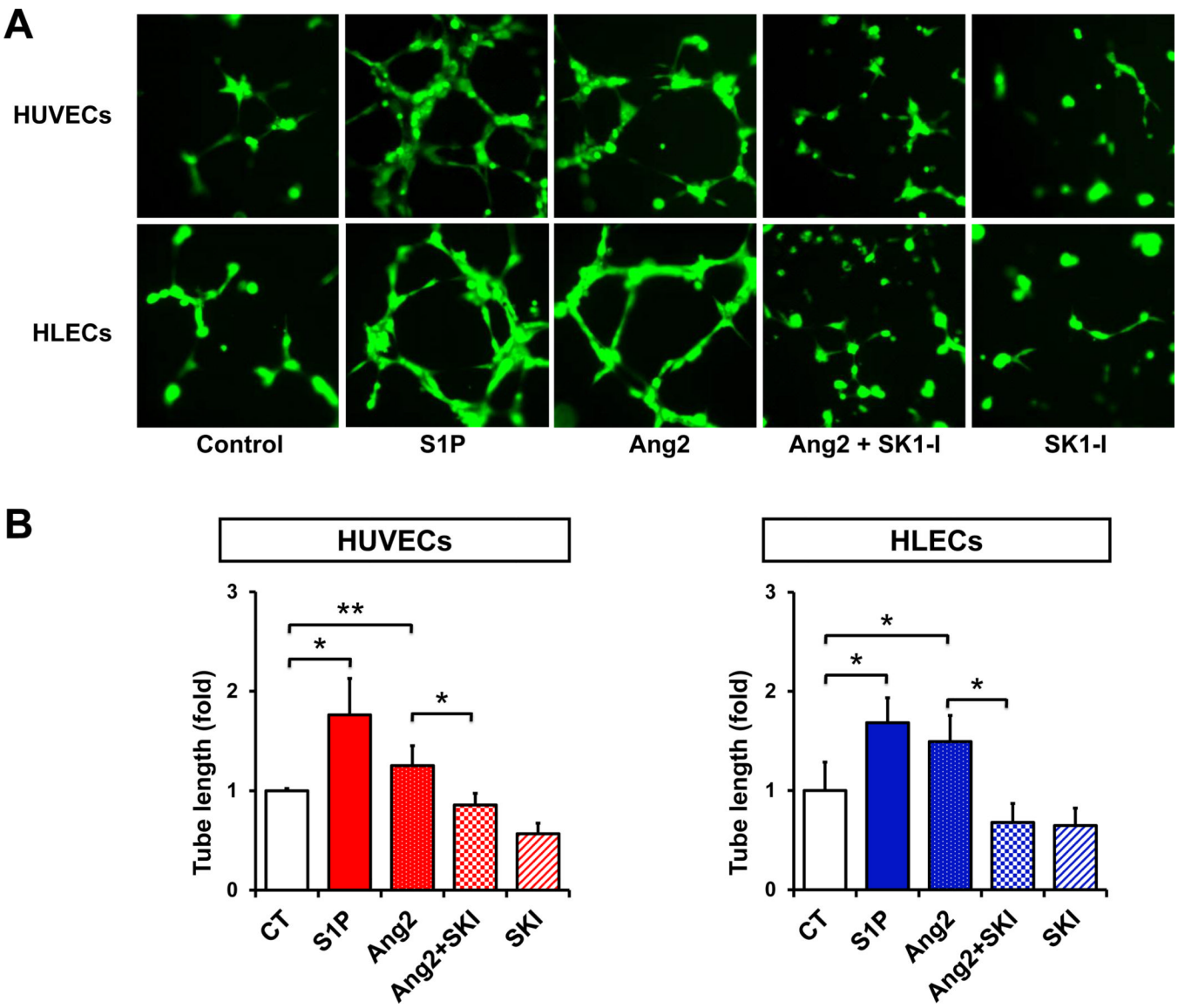

Figure 4. Inhibition of SphK1 suppresses *in vitro* hemangiogenesis and lymphangiogenesis

GFP expressing HUVECs and HLECs were cultured on reduced growth factor basement membrane matrix-coated 48 well plates and incubated for 6 hours with or without S1P (1 μM), Ang2 (500 ng/ml), or SK1-I (10 μM), as indicated. (A) Representative images. (B) Two random fields per well were photographed. Total tube length determined and means ± SD are shown. *, $P < 0.01$; **, $P < 0.05$.

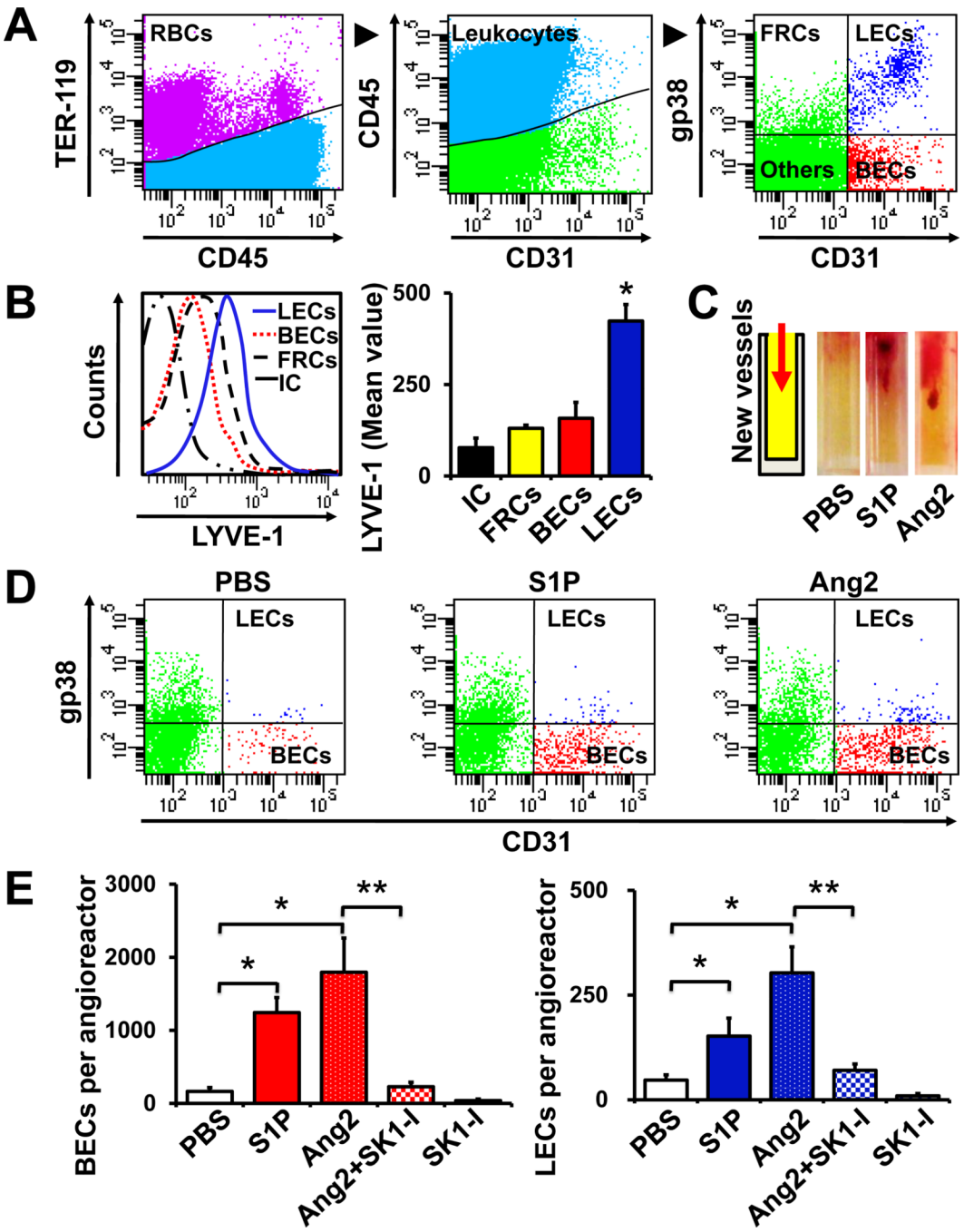

Figure 5. Inhibition of SphK1 suppresses hemangiogenesis and lymphangiogenesis quantified by DIVAA/FACS

(A, B) FACS gating scheme to quantify blood endothelial cells (BEC) and lymphatic endothelial cells (LEC) from the same lymph node single cell suspension. (A) TER-119 and CD45 were used to gate out the RBCs and lymphocytes, respectively. CD31 and gp38 (podoplanin) expression allowed separation of LECs and BECs from other TER-119^{-}CD45^{-} cells: fibroblastic reticular cells (FRCs) and double-negative stromal cells (Others). (B) LYVE-1 expression on the indicated populations or isotype control (IC) on the total population was quantified by FACS and mean values ± SEM are shown in the right panel. *, $P < 0.001$. (C-E) Quantification of BECs and LECs by DIVAA/FACS. (C)

Angioreactors are closed at bottom end and filled with 20 μl of Matrigel. Addition of stimuli in the Matrigel enables directional migration of BECs and LECs into the angioreactors, which proliferate and form appropriate vessels (left). Hemangiogenesis was readily observable by the appearance of blood vessels in the angioreactors containing S1P (1 μM), or Ang2 (1 μg/ml) compared to PBS. (D) Cells were isolated from the angioreactors and BECs and LECs were analyzed by FACS with antibodies to TER-119, CD45, CD31 and gp38 as in (A). (E) Total number of BECs and LECs were calculated and means ± SEM are shown. *, $P < 0.01$; **, $P < 0.05$.

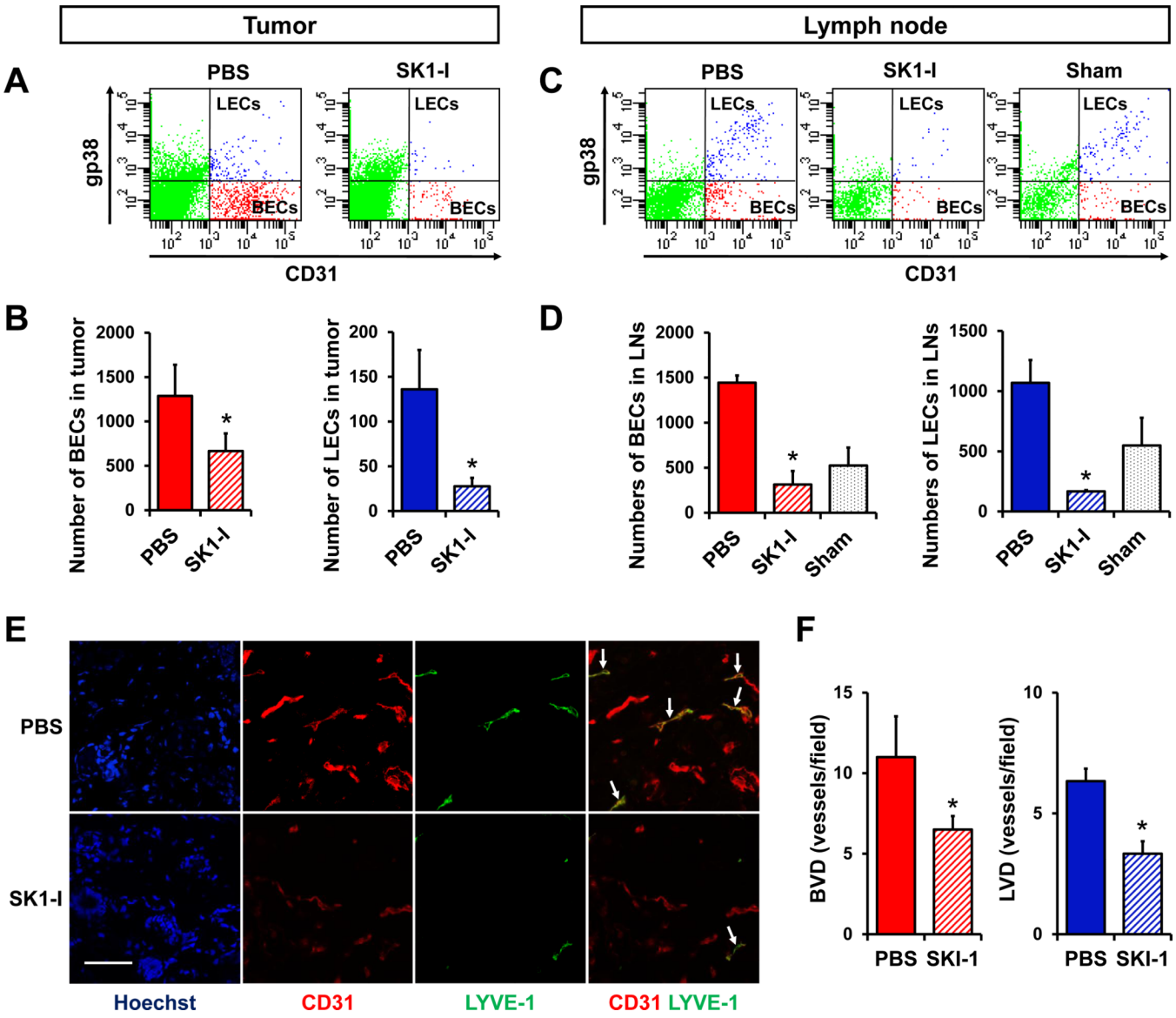

Figure 6. Inhibition of SphK1 suppresses hemangiogenesis and lymphangiogenesis in tumors and lymph nodes *in vivo*

4T1-luc2 cells implanted in chest mammary fat pads were allowed to form tumors for 2 days, which were quantified by IVIS. Mice with similar amounts of tumor were randomized and treated with either PBS or SK1-I (20mg/kg/day i.p.). Tumors (A, B) and regional axillary lymph nodes (C, D) were harvested after 4 days of treatment, minced, digested with collagenase, and BECs and LECs quantified by FACS. Total numbers of BECs or LECs in 4T1 tumors (B) and lymph nodes (D) are shown as means ± SEM. * $P < 0.05$. (E) Immunofluorescent staining for CD31 and LYVE-1. $CD31^{+}LYVE\text{-}1^{-}$ cells were considered as blood vessels, $CD31^{+}LYVE\text{-}1^{+}$ cells as lymphatic vessels (arrows). (F) Morphometric analysis of blood and lymphatic vessel densities were determined in the peritumoral regions after 7 days of treatment, and are shown as means± SEM. *, $P < 0.05$. Scale bar, 50 μm.